ELSEVIER

Contents lists available at ScienceDirect

### International Journal of Biological Macromolecules

journal homepage: www.elsevier.com/locate/ijbiomac





## Synthesis of multivalent sialyllactose-conjugated PAMAM dendrimers: Binding to SARS-CoV-2 spike protein and influenza hemagglutinin

Peng He <sup>a,b</sup>, Ke Xia <sup>a,b</sup>, Yuefan Song <sup>a,b</sup>, Ritesh Tandon <sup>c</sup>, Rudra Channappanavar <sup>d</sup>, Fuming Zhang <sup>b,e,\*</sup>, Robert J. Linhardt <sup>a,b,e,\*</sup>

- <sup>a</sup> Department of Chemistry and Chemical Biology, Rensselaer Polytechnic Institute, Troy, NY 12180, USA
- <sup>b</sup> Center for Biotechnology and Interdisciplinary Studies, Rensselaer Polytechnic Institute, Troy, NY 12180, USA
- <sup>c</sup> Center for Immunology and Microbial Research, Department of Cell Biology, Medicine and BioMolecular Sciences, University of Mississippi Medical Center, Jackson, MS USA
- d Department of Veterinary Pathobiology, Oklahoma Center for Respiratory and Infectious Diseases (OCRID), Oklahoma State University, Stillwater, OK, USA
- e Department of Chemical and Biological Engineering, Rensselaer Polytechnic Institute, Troy, NY 12180, USA

#### ARTICLE INFO

# Keywords: Sialyl glycoconjugate 6'-Sialyllactose-counjugated polyamidoamine dendrimers Click chemistry SPR SARS-CoV-2 Spike protein Human influenza A Influenza hemagglutinin

#### ABSTRACT

Severe acute respiratory syndrome-related coronavirus-2 (SARS-CoV-2) and influenza viruses have spread around the world at an unprecedented rate. Despite multiple vaccines, new variants of SARS-CoV-2 and influenza have caused a remarkable level of pathogenesis. The development of effective antiviral drugs to treat SARS-CoV-2 and influenza remains a high priority. Inhibiting viral cell surface attachment represents an early and efficient means to block virus infection. Sialyl glycoconjugates, on the surface of human cell membranes, play an important role as host cell receptors for influenza A virus and 9-O-acetyl-sialylated glycoconjugates are receptors for MERS, HKU1 and bovine coronaviruses. We designed and synthesized multivalent 6'-sialyllactose-counjugated polyamidoamine dendrimers through click chemistry at room temperature concisely. These dendrimer derivatives have good solubility and stability in aqueous solutions. SPR, a real-time analysis quantitative method for of biomolecular interactions, was used to study the binding affinities of our dendrimer derivatives by utilizing only 200 micrograms of each dendrimer. Three SARS-CoV-2 S-protein receptor binding domain (wild type and two Omicron mutants) bound to multivalent 9-O-acetyl-6'-sialyllactose-counjugated and 6'-sialyllactose-counjugated dendrimers bound to a single H3N2 influenza A virus's HA protein (A/Hong Kong/1/1968), the SPR study results suggest their potential anti-viral activities.

#### 1. Introduction

The variants of severe acute respiratory syndrome-related corona-virus-2 (SARS-CoV-2) continue to arise at an unprecedented rate, leading to the global pandemic we now face [1,2]. More than 6 million people have been killed by SARS-CoV-2 worldwide since 2019 and these numbers are still rising [3]. Influenza viruses, family members of Orthomyxoviridae, comprise influenza A, B, C and D four genera (IVA, IVB, IVC and IVD). Among these, IVAs are the major cause of human annual epidemic and occasional pandemic influenza diseases [4,5]. Both SARS-CoV-2 and IVAs are characterized by respiratory symptoms, including runny nose, fever, sore throat, cough, and breathing difficulties [6,7]. Hemagglutinin (HA) and neuraminidase (NA), found on the surface of IVAs, are integral to their infectivity. IVAs are also

classified by HA (H) and NA (N) (HxNy, x is 1 through 18 and y is 1 through 11, respectively). Many chemical and biological anti-influenza drugs use HA and NA proteins as the treatment target [8]. The binding of HA from human IVAs to sialoglycans on the host cell surface starts the IVA infection cycle and  $\alpha$ -2,6-sialoglycans are preferred ( $\alpha$ -2,3-sialoglycans are preferred by avian influenza viruses) [9,10].

Spike protein plays a critical role in SARS-CoV-2 infection. The binding of SARS-CoV-2 spike protein to host's mucus membranes through angiotensin-converting enzyme 2 (ACE2) receptor is a critical initial step for viral infection [11]. Evidence suggests the importance of acidic glycans (i.e., acidic heparan sulfate polysaccharides, sialoglycans, etc.) as co-receptors [12,13]. Sialoglycans reportedly facilitate viral entry of several types of human coronaviruses. For example, the spike protein of Middle East respiratory syndrome coronavirus (MERS-CoV) is

<sup>\*</sup> Corresponding authors at: Center for Biotechnology and Interdisciplinary Studies, Rensselaer Polytechnic Institute, Troy, NY 12180, USA. E-mail addresses: zhangf2@rpi.edu (F. Zhang), linhar@rpi.edu (R.J. Linhardt).

known to bind to  $\alpha$ -2,3-linked (and to  $\alpha$ -2,6-linked to a lesser extent) sialic acids [14]. The spike proteins domain A of human coronavirus (HCoV) OC43 and HKU1 bind to 9-O-acetylated sialoglycans. Studies show that 9-O-acetyl sialic acid binding sites of several coronaviruses (i. e., HCoV-OC43, HCoV-HKU1, and BCov) are highly conserved [15]. Recent evidence suggests that sialogylcans also can act as an ACE2 coreceptor-binding domain for SARS-CoV-2 spike protein. A series of sialoglycans have been applied for testing the binding with SARS-CoV-2 spike protein. Some of the sialoglycans showed a weak binding with the spike protein (such as α-2-3-linked Neu5Ac, 9/4-O-acetyl Neu5Ac, and 9-N-acetyl Neu5Ac) [16]. Alexander and coworkers reported a series of gold nanoparticles bearing Neu5Ac which showed specific binding towards SARS-CoV-2 spike protein S1 domains over the SARS-COV-1 spike protein [17]. Several multimeric 9-O-acetyl sialic gylcoclusters were synthesized and tested the binding affinity to purified SARS-CoV-2 S1 protein and its virions, the results showed that these glycoclusters had binding affinities and could facilitate their use as potent SARS-CoV-2 inhibitors [18].

Although several types of antiviral vaccines have been developed to prevent SARS-CoV-2 and IVA, emerging variants have severely limited vaccine efficacy and immune escape [19,20]. Novel effective antiviral drugs against SARS-CoV-2 and IVA are in incredibly high demand. Polyamidoamine (PAMAM) dendrimers are attractive templates for the design of multivalent clusters for use against virus infections. Our group reported that a series of multivalent 6'-sialyllatose PAMAM dendrimer nanostructured conjugates showed optimal inhibition of H1N1 influenza A virus infection through multivalent binding to viral hemagglutinin trimer [21]. Sialyllactose-PAMAM dendrimer multivalent polymers can act as both human and avian influenza virus inhibitors as confirmed in cell neutralization assays [22]. Sialyllactose-conjugated PAMAM dendrimers possess excellent solubility, stability, and multivalent binding capabilities. The well-defined PAMAM dendrimer G1 architecture enables the display of multiple sialyllactose moieties on the dendrimer surface, show promising enhanced interactions with viral proteins or receptors, potentially leading to the competitive inhibition of viral

attachment to host cells. Moreover, such defined glycodendrimers facilitate the quantitative determination and comparison of binding affinities to different viral receptor proteins.

In this work, we present a simple and efficient design and synthesis of multivalent 6'-sialyllatose-PAMAM dendrimer derivatives 1, 2, 3 and 4 (Fig. 1). First, the surface of PAMAM dendrimer G1 was modified with an alkynyl group. Simultaneously, 6'-sialyllactose azide and 9-acetyl-6'-sialyllactose azide were synthesized. Then, a straightforward and efficient click chemistry method was employed to conjugate the sialyllactose azide onto the surface of the PAMAM dendrimer. Surface plasmon resonance (SPR) was applied to investigate the biophysical properties (e.g., real time affinity, association constant and dissociation constant) of these multivalent 6'-sialyllactose derivatives to SARS-CoV-2 spike proteins and HA proteins. We show that SARS-Cov-2 S proteins and H3N2 HA protein can be inhibited by 9-acetyl-6'-sialyllactose conjugated PAMAM dendrimer and 6'-sialyllactose conjugated PAMAM dendrimer, respectively. The results also indicate that 9-O-acteyl group will play an important role in the different viral inhibition activities.

#### 2. Results and discussion

#### 2.1. Chemistry

Biotinylated multivalent 9-O-acetylated sialyllatose-PAMAM dendrimer G1 1 and sialyllatose-PAMAM dendrimer G1 2 were first synthesized. The trisaacharide 6'-sialyllactose was initially converted at its reducing end to its azido derivative, which enabled the efficient conjugation to alkyne group. Different strategies were developed to introduce an azido moiety to the anomeric position of sugars. The normal protection and deprotection multi-step synthetic strategy is time consuming and is difficult to apply to oligosaccharides. Thus, the direct activation of anomeric hydroxy group of unprotected sugars in aqueous media was employed. 2-Chloro-1,3-dimethylimidazolinium chloride (DMC) proved to be a powerful anomeric activating agent of unprotected sugars in aqueous media. The enhanced acidity of carbohydrate's anomeric

Fig. 1. Designed multivalent 6'-sialyllatose-PAMAM dendrimer derivatives.

hydroxyl group (pKa range  $\sim 12.1-12.5$ ) makes it possible to selectively activate it with DMC under basic reaction conditions. The DMCactivated unprotected sugars can undergo reactions with different nucleophiles, providing short and efficient routes to corresponding glycosides and glycoconjugates [23]. Azide, aryl thiol, phenol and thiosulfate have been proved to be suitable nucleophiles to prepare the corresponding glycosides from unprotected sugars in one or two steps [24]. As outlined in Scheme 1, 9-O-acetylated-6'-sialyllactosyl azide 7 was synthesized for the conjugation with alkyne groups through the CuAAC reaction. 6'-Sialyllactose was directly converted into the corresponding 6'-sialyllactosyl azide 6 using DMC as the activator and DIPEA in aqueous basic solution. Several reports describe the regioselective chemical synthesis of 9-O-acetylation of Neu5Ac from unprotected Neu5Ac [25-27]. 9-O-Acetylation Neu5Ac has been carried out by the treatment of trimethyl orthoacetate and catalytic amount of p-TsOH in anhydrous DMSO. Treatment with our 6'-sialyllactosyl azide 6 with 2.5 equiv. trimethyl orthoacetate and 0.1 equiv. p-TsOH successfully afforded 9-O-acetyl-6'-sialyllactosy azide 7. The purification of 7 was carried out with a Shimadzu HPLC system equipped with an Agilent Poroshell 120 EC-C<sub>18</sub> column (3.0  $\times$  150 mm, 2.7  $\mu$ m). The introduction of 9-O-acetyl group results in the shift of the proton of C9 in the sialic residue changing from 3.4 to 3.5 ppm to 3.85–4.0 ppm in <sup>1</sup>H NMR spectrum, at same time the shift of the carbon of C9 in the sialic residue changes from 62.34 ppm to 65.41 ppm <sup>13</sup>C NMR spectrum. The 9-Oacetyl group was confirmed with 1D NMR and 2D NMR (Figs. S1-S10, <sup>1</sup>H and <sup>13</sup>C, COSY, HSQC and HMBC spectra).

Biotinylated multivalent 9-O-acetylated-sialyllatose-PAMAM dendrimer G1 1 designed for this study are based on a generation 1 PAMAM dendrimer. A biotin-PEG<sub>12</sub> arm was introduced to PAMAM G1 through condensation of carboxyl group and amino group to immobilize dendrimer compound to the SA chip for SPR analyses (Scheme 2). Carboxylic acids can be prepared as active esters and acylimidazoles with different condensing agents, such as dicyclohexyl carbodiimide (DCC), N-(3-dimethylaminopropyl)-N'-ethylcarbodiimide (EDC), and carbonyl diimidazole (CDI), etc. At the same time N-hydroxysuccinimide (NHS), 1-hydroxy-1H-benzotriazole (HOBt), 1-hydroxy-7-azabenzotriazole (HOAt) are used as additives. Since there are 8 amine groups arms in the periphery of PAMAM G1, precise control of mole ratio of biotinylated linker and PAMAM G1 is very important. Hence, well prepared

biotin-PEG<sub>12</sub>-NHS ester was chosen as the source of biotinylated arm, which is an easy-weighting and water-soluble white solid. The biotin-PEG<sub>12</sub>-NHS reacted efficiently with one of peripheral amine group of PAMAM G1 in PBS buffer (pH 7.2) with a molar ratio of 1/2 (Biotin-PEG<sub>12</sub>-PAMAM G1, 75 % yield). The purification of biotinylated PAMAM G1 was performed using Shimadzu gel permeation chromatography (GPC) system equipped with a Superdex TM 30 increase 10/ 300 GL size exclusion column. 4-Pentynoic acid was employed as the alkyne source for the synthesis of biotinylated alkynyl-PAMAM-G1 9 with 7 peripheral alkyne arms for the CuAAC reaction. Different condensation methods (i.e., TATU, HBTU, EDCI/NHS, and DMTMM) were examined to obtain fully alkynylation biotin-PAMAM G1 9. DMTMM, without adjusting reaction pH, was found the most effective coupling agent to obtain the fully alkynylated product. An excess of 4pentynoic acid and DMTMM were employed to ensure the functionalization of the additional 7 dendrimer amino arms were totally modified with alkyne. Since all the reagents are water soluble, the biotinylated alkynyl 9 was simply purified by centrifugation with a Microsep Advance 1K Yellow Omega (1K Da cut off) centrifugal device. The structure of **9** was confirmed by the nuclear magnetic resonance (NMR) spectroscopy and electrospray ionization (ESI) mass spectrometry (MS).

The synthesis of entire periphery alkynyl PAMAM G1 10 was conducted using the same DMTMM condensation method. The coupling of 4-pentynioc acid and PAMAM dendrimer G1 was carried out using DMTMM as the coupling reagent. The purification of 10 used a Superdex<sup>TM</sup> 30 Increase 10/300 GL column on Shimadzu HPLC system. The structure of 10 was confirmed by the NMR and ESI-MS.

The CuAAC reaction is a cornerstone method for the selective conjugation of different molecules in a high yield, high purity, using green chemistry and atomic economy [27,28]. Click chemistry conjugation of 9 with azide 7 was performed in water in the presence of CuSO<sub>4</sub> and sodium L-(+)-ascorbate. The results showed that the surface alkynes of biotinylated 9 were not fully conjugated with azide 7 under N<sub>2</sub> protection. Water-soluble tris(3-hydroxypropyl-triazolylmethyl) amine (THPTA) is an outstanding. Cu(I)-stabilizing ligand that can keep Cu(I) active longer and make the cycloaddition reaction more efficient [29]. The addition of THPTA in our rection improved the azide-alkyne reaction, affording the fully armed biotinylated 1. The multivalent PAMAM dendrimer 2, 3 and 4 were synthesized using the same protocol.

Scheme 1. Synthesis of 9-O-acetylated-6'-sialyllatosyl azide.

Scheme 2. Synthesis of multivalent 9-O-acetylated-6'-sialyllatose-PAMAM dendrimer G1<sup>a</sup>.eagents and conditions: (a) i) NHS-PEG<sub>12</sub>-Bition, PBS buffer pH 7.2; ii) 4-pentynioc acid, DMTMM, H<sub>2</sub>O, 65 % for two steps; (b) 4-pentynioc acid, DMTMM, H<sub>2</sub>O, 86 %; (c) CuSO<sub>4</sub>, sodium L-(+)-ascorbate, H<sub>2</sub>O, 91 %.

# 2.2. Binding affinity and kinetics measurement of sialyllactose-dendrimer with SARS-CoV-2 S protein and H2N3 IVA HA protein

SPR is an excellent technique providing real-time data on biomolecular interactions, including the association rate (ka), dissociation rate (kd) and binding constant ( $K_D$ ) [30]. Series S Sensor SA is a widely used SPR biosensor chip, consisting of a pre-immobilized streptavidin surface for the fast and high-affinity capture of biotinylated molecules [31]. In the current study, the biotinylated 1 and 3 are first non-covalently immobilized on the Series S Sensor Chip SA to measure their binding kinetics and affinities for SARS-CoV-2 spike protein RBD and  $H_2N_3$  IVA HA.

The interaction of biotinylated 1 and 3 with SARS-CoV-2 Spike protein RBD (wild type (wt), Omicron BA4 mutant, Omicron BA5 mutant) were first examined by SPR on a Biacore T200 system (GE, Healthcare, Uppsala, Sweden) (Fig. 2). Biotin was used as a negative control. Briefly, biotin, biotinylated 1 and 3 were each immobilized to a flow cell of a Series S Sensor SA based on the manufacturer's protocol. Successful immobilization of biotinylated samples was confirmed by the observation of a >500-resonance unit (RU) increase in the sensor chip. Different dilutions of corresponding SARS-CoV-2 spike protein, dissolved in HBS-EP plus pH 7.4 buffer (0.01 M 4-(2-hydroxyethyl)-1-piperazineethanesulfonic acid, 0.15 M NaCl, 0.003 M ethylenediaminetetraacetic acid and 0.05 %  $\nu/\nu$  surfactant P20), were injected over the sensor surface a flow rate of 30  $\mu$ L/min. The sensor surface was dissociated with the same buffer at the end of each injection,

then regenerated by injecting 30  $\mu L$  of 2 M aqueous NaCl. All the sensorgrams were monitored at 25  $^{\circ} C.$  Since the 9-O-acetyl group of 9-O-acetylated-6′-sialyllactosyl dendrimer can be cleaved under strongly basic or acidic conditions and the acetyl group can migrate under weakly basic conditions, our SPR studies were performed under physiological conditions at around pH 7.

The SPR results demonstrated that the multivalent 9-O-acetylated-6'-sialyllactosyl dendrimer 1 exhibited a high binding affinity for Spike protein of three SARS-CoV-2 subtypes ( $K_D=110$  to 490 nM) (Table 1). The multivalent 6'-sialyllactosyl dendrimer 3 shows no interaction with any of these spike proteins indicating that the presence of a 9-O-acetyl group on sialic residues is critical for binding the spike protein of SARS-CoV-2. These results indicated that 9-O-acetylated-6'-sialyllacotse residues rather than 6'-sialyllacotse residues can act as a co-receptor or attachment factors for the SARS-CoV-2 spike protein.

Among the four types of influenza viruses (A, B, C and D), IVA are the only influenza viruses that can cause annual flu epidemics and global pandemics. IVAs subtypes  $\rm H_1N_1$  and  $\rm H_3N_2$  routinely circulate in people and are responsible for a series of deadly flu pandemics. The HA of IAV binds to specific terminal sialylated glycans residues. HA derived from human-adapted IAV binds specifically to a  $\alpha$ -2-6 sialylated glycans whereas avain-adapted species prefer  $\alpha$ -2-3 sialylated glycans. Several studies showed that multivalent sialic acid glycoclusters exhibit promising inhibition activity towards  $\rm H_1N_1$  and  $\rm H_3N_2$  IVA. Miura and coworkers reported various glycopolymers bearing  $\alpha$ -2-6-sialyllactose showed specific binding to  $\rm H_3N_2$  (A/Aichi/2/68 IVA strain) but showed

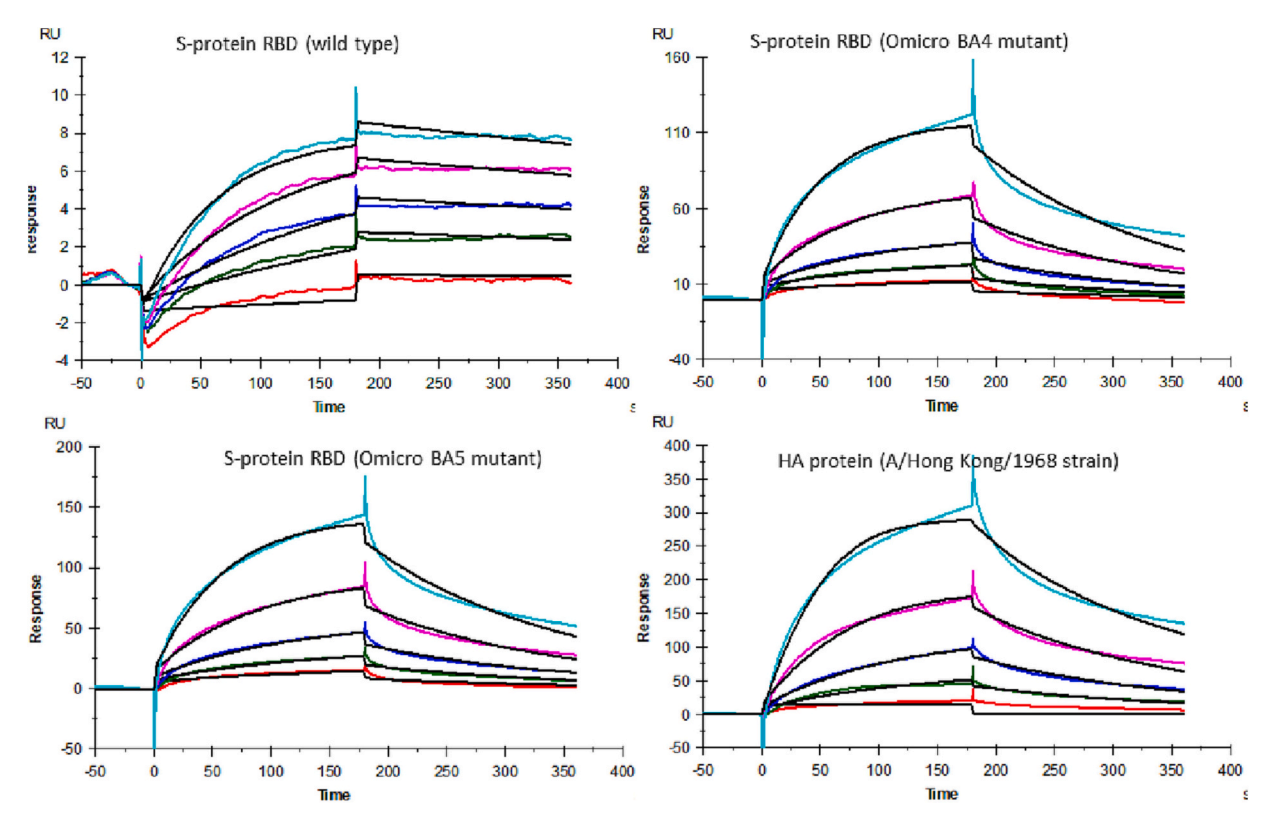


Fig. 2. SPR sensorgrams of SARS-CoV-2 spike protein (wild type (wt), Omicron BA4 and Omicron BA5 mutant) binding with multivalent 9-O-acetylated-6'-sialyllactose PAMAM dendrimer 1. The protein concentrations are 2000, 1000, 500, 250, and 125 nM (from top to bottom), respectively. (B) SPR sensorgram and kinetics of HA binding to 6'-sialyllactose PAMAM dendrimer 3. The protein concentrations are 1000, 500, 250, 125, and 63 nM (from top to bottom), respectively. The black curves are the Langmuir 1:1 kinetic fitting using models from Biacore T200 evaluation software

**Table 1**Summary of kinetic parameters for SARS-CoV-2 spike protein RBD (wt and mutants) and HA protein (A/Hong Kong/1/1968 stain) with multivalent sialyllatose-PAMAM dendrimer 1 and 3 interactions.

Interactions	$k_a$ (M $^{-1}$ s $^{-1}$ )	$k_{\rm d}$ (s <sup>-1</sup> )	K <sub>D</sub> (M)
SARS-CoV-2 spike protein RBD (wt) with compound 1	$7.3 \times 10^{3}$ (±140)	$8.1 \times 10^{-4}$ ( $\pm 1.6 \times 10^{-5}$ )	$1.1 \times 10^{-7}$ (±2.4 × $10^{-8}$ ) <sup>a</sup>
SARS-CoV-2 spike protein RBD (Omicron BA4) with compound 1	$1.334 \times 10^{3} \ (\pm 120)$	$6.5 \times 10^{-3}$ ( $\pm 2.7 \times 10^{-5}$ )	$4.9 \times 10^{-7}$ $(\pm 3.1 \times 10^{-8})^{a}$
SARS-CoV-2 spike protein RBD (Omicron BA5) with compound 1	$1.0 \times 10^{3}$ (±460)	$4.7 \times 10^{-3}$ ( $\pm 7.5 \times 10^{-5}$ )	$4.6 \times 10^{-7}$ $(\pm 1.7 \times 10^{-8})^{a}$
HA protein (A/Hong Kong/1/1968 strain) with compound 3	$3.2 \times 10^4$ (±740)	$7.6 \times 10^{-3}$ ( $\pm 1.1 \times 10^{-4}$ )	$3.0 \times 10^{-7}$ (±2.6 × $10^{-8}$ ) <sup>a</sup>

The data with  $(\pm)$  in parentheses are the standard deviations (SD) from global fitting of five injections using a 1:1.

no interaction with  $H_1N_1$  stains. Some studies also found that the  $\alpha$ -2-6-sialyllactose multivalent conjugates only show some binding with HA derived from  $H_3N_2$  IVA. In the current study, we utilized SPR to measure the binding of three  $H_1N_1$  HA and three  $H_3N_2$  HA with our two biotinylated dendrimer 1 and 3. The results showed that only 3 showed good binding and only with  $H_3N_2$  (A/Hong Kong/1/1968). Biotinylated dendrimer 3 showed no binding with any of the HA proteins tested. The results indicate that HA of this  $H_3N_2$  (A/Hong Kong/1/1968) can utilize  $\alpha$ -2-6-sialyllactose as a receptor determinant. The 9-0-acetylation of sialic residue abolishes the binding ability with the HA of this  $H_3N_2$  IVA.

#### 3. Conclusion

We present a brief and efficient method to synthesize a biotinylated 9-O-acetylated-6'-sialyllatose-PAMAM dendrimer 1 and biotinylated sialyllatose-PAMAM dendrimer 3. SPR studies revealed that biotinylated multivalent 9-O-acetylated-6'-sialyllactose dendrimer 3 showed tight binding to SARS-CoV-2 spike protein (110 to 490 nm), whereas no interaction was observed with HA of IVA. Biotinylated 6'-sialyllatose-PAMAM dendrimer 3 showed tight binding with HA of H<sub>3</sub>N<sub>2</sub> (A/Hong Kong/1/1968 stain), whereas no binding with any tested SARS-CoV-2 spike protein. Our results reveal that mutivalent 9-O-acetylated-6'-sialyllatose-PAMAM dendrimer can act as an attachment factor when SARS-CoV-2 binds to host cell surface. But the hydroxyl group at the 9 position of the sialic acid residue plays a critical role in the interaction with HA of H<sub>3</sub>N<sub>2</sub> IVA. This selectivity might be useful for developing therapeutic or diagnostic approaches for these respiratory infections. Our study showed that our sialyllactose-conjugated dendrimer derivatives are good inhibitors towards the important key viral proteins (S protein and HA proteins) which play a crucial role in the infectivity and pathogenicity of the related viruses. Further in vivo investigation on the antiviral activity of these dendrimers is underway to confirm their antiviral activities. These multivalent sialyllactose derivatives PAMAM dendrimers enhance binding avidity and represent promising candidates for developing inhibitors for SARS-CoV-2 and influenza infection.

#### 4. Experimental section

#### 4.1. Chemistry

#### 4.1.1. General information

All reagents were purchased from Millipore Sigma (Burlington, MA,

<sup>&</sup>lt;sup>a</sup> Standard deviation on triplicate experiments.

USA) such as PAMAM dendrimer G1, 6'-Sialyllactose sodium, sodium azide etc., and unless noted otherwise, used without further purification. Flash chromatography (FC) was performed using silica gel (200–400 mesh; MilliporeSigma, Burlington, MA, USA) according to standard protocols. Reactions were monitored by thin-layer chromatography (TLC) on silica gel F254 plates (20 cm  $\times$  20 cm, MilliporeSigma, Burlington, MA, USA). Mass data were acquired by electrospray ionization (ESI)-high-resolution (HR)-MS on an LTQ-Orbitrap XL FT-MS spectrometer.  $^{1}\mathrm{H},~^{13}\mathrm{C}$  nuclear magnetic resonance spectroscopy (NMR) spectra were recorded on an 800 MHz (200 MHz for  $^{13}\mathrm{C}$  NMR) spectrometer.

#### 4.1.2. Synthesis

4.1.2.1. Synthesis of 6'-sialyllactosyl azide (6). To a solution of 6'-sialyllactose (10 mg, 15.8 μmol) in 2 mL water was added NaN<sub>3</sub> (19.5 mg, 0.3 mmol), 2-chloro-1,3-dimethylimidazolinium chloride (DMC) (25.4 mg, 0.15 mmol) and N, N-diisopropylethylamine (78  $\mu$ L, 0.45 mmol). The resulting solution was stirred vigorously for 12 h at rt. The reaction mixture was evaporated and dissolved in water, then the solution was purified by Superdex<sup>TM</sup> 30 increase size exclusion chromatography column to give of 6'-sialyllactosyl azide **6** as a white solid. (9.4 mg, 90 %). <sup>1</sup>H NMR (800 MHz, <sup>2</sup>H<sub>2</sub>O)  $\delta$  4.53 (dt, J = 7.4, 3.3 Hz, 1H), 4.18 (t, J= 5.2 Hz, 1H, 3.73 (dd, J = 12.3, 4.3 Hz, 2H, 3.69 (s, 1H), 3.67-3.56(m, 5H), 3.48 (dd, J = 11.2, 3.6 Hz, 1H), 3.42 (dt, J = 28.1, 5.9 Hz, 6H),3.36-3.27 (m, 3H), 3.12-3.08 (m, 1H), 2.51-2.44 (m, 1H), 1.80-1.77 (m, 3H), 1.50 (td, J = 13.1, 12.1, 3.2 Hz, 1H). <sup>13</sup>C NMR (200 MHz, D<sub>2</sub>O)  $\delta$  174.64, 173.36, 102.98, 100, 89.58, 78.72, 76.29, 74.35, 73.48, 72.28, 72.18, 72.05, 71.61, 70.51, 68.26, 68.21, 68.1, 63.45, 62.34, 59.69, 51.51, 39.88, 21.81. ESI-HRMS calcd. for C<sub>23</sub>H<sub>37</sub>N<sub>4</sub>O<sub>19</sub> ([M - H]<sup>-</sup>) 657.2108, found 657.2114.

4.1.2.2. Synthesis of 9-O-acetylated-6'-sialyllactosyl azide (7). To a solution of 6 (10 mg, 15.2  $\mu$ mol) in 0.2 mL dimethyl sulfoxide was added trimethyl orthoacetate (6 µL, 53 µmol), and p-toluenesulfonic acid monohydrate (1.1 mg,  $6 \mu mol$ ). The mixture was stirred vigorously for  $6 \mu mol$ h at rt. Then NH<sub>4</sub>HCO<sub>3</sub> 4 mg was added to quench the reaction. The reaction mixture was evaporated and dissolved in water, then residues were purified using a reversed-phase high performance liquid chromatography (HPLC) instrument (Shimadzu, Kyoto, Japan) equipped with an SPD-M40 photo diode array detector (Shimadzu, Kyoto, Japan) and an Agilent Poroshell 120 EC-C18 column (2.7 mm,  $4.6 \times 250$  mm), using 50 mM NH<sub>4</sub>HCO<sub>3</sub> water/acetonitrile = 95/5 ( $\nu$ /v) as the mobile phase, at a flow rate of 0.3 mL/min to afford 7 as a white solid powder (8.6 mg, 81 %). <sup>1</sup>H NMR (800 MHz, <sup>2</sup>H<sub>2</sub>O)  $\delta$  4.54 (dd, J = 9.2, 5.2 Hz, 1H), 4.17 (dd, J = 12.3, 4.6 Hz, 1H), 3.95 (dd, J = 11.8, 5.6 Hz, 1H), 3.88 (ddd, J)= 8.8, 5.9, 2.7 Hz, 1H), 3.73 (p, J = 4.8 Hz, 1H), 3.69 (d, J = 3.7 Hz, 1H),3.66-3.55 (m, 3H), 3.52 (d, J = 10.9 Hz, 1H), 3.48-3.26 (m, 5H), 3.13-3.07 (m, 1H), 2.46 (dd, J = 12.7, 4.9 Hz, 1H), 1.89 (d, J = 5.5 Hz, 3H), 1.79 (d, J = 5.8 Hz, 3H), 1.50 (dd, J = 14.1, 10.2 Hz, 1H). <sup>13</sup>C NMR (200 MHz,  ${}^{2}\text{H}_{2}\text{O}$ )  $\delta$  174.59, 174.17, 173.34, 102.98, 100.02, 89.57, 78.77, 76.28, 74.33, 73.54, 72.18, 72.05, 70.47, 69.03, 68.3, 68.23, 68.08, 65.41, 63.6, 59.69, 51.48, 39.9, 21.84, 20.04. ESI-HRMS calcd. For  $C_{25}H_{39}N_4O_{19}^-$  ([M - H]<sup>-</sup>) 699.2214, found 699.2142.

4.1.2.3. Synthesis of biotinylated alkynyl-PAMAM dendrimer (9). To a solution of PAMAM dendrimer G1 (80 mg, 56  $\mu$ mol) in 400  $\mu$ L PBS buffer (pH 7.2) was added biotin-PEG12-NHS ester (26 mg, 28  $\mu$ mol). The resulting solution was stirred vigorously for 12 h at 4 °C. The reaction buffer was changed to 1 mL water with 1K Macrosep Advance centrifugal device. Then 4-pentynoic acid (132 mg, 1.4 mmol) and DMTMM (775 mg, 2.8 mmol) were added to reaction mixture, the mixture was stirred for 12 h at rt. The solution was purified by Superdex M 30 increase size exclusion chromatography column to give of biotinylated PAMAM 9 as a white solid (102 mg, 65 % for two steps).  $^1$ H NMR (800

MHz,  $^2\mathrm{H}_2\mathrm{O})$   $\delta$  8.20 (s, 1H), 4.36 (dd, J=8.0, 4.9 Hz, 1H), 4.18 (dd, J=8.0, 4.4 Hz, 1H), 3.53 (t, J=6.1 Hz, 2H), 3.49–3.42 (m, 46H), 3.38 (t, J=5.3 Hz, 2H), 3.15 (t, J=5.3 Hz, 2H), 3.12–3.04 (m, 42H), 2.75 (dd, J=13.1, 5.0 Hz, 1H), 2.62–2.51 (m, 26H), 2.42–2.34 (m, 12H), 2.28 (t, J=6.1 Hz, 2H), 2.25–2.22 (m, 16H), 2.21–2.15 (m, 38H), 2.03 (t, J=7.3 Hz, 2H), 1.55–1.28 (m, 4H), 1.20–1.13 (m, 2H).  $^{13}\mathrm{C}$  NMR (200 MHz,  $^2\mathrm{H}_2\mathrm{O})$   $\delta$  174.77, 174.62, 174.25, 173.93, 170.86, 82.46, 69.4, 61.88, 60.04, 55.19, 50.91, 49.73, 48.85, 48.72, 39.53, 38.54, 38.29, 36.5, 34.3, 32.38, 32.26, 14.37. ESI-HRMS calcd. for  $\mathrm{C}_{134}\mathrm{H}_{224}\mathrm{N}_{29}\mathrm{O}_{72}\mathrm{S}$  ([M + H] $^+$ ) 2815.6406, found 2815.6674.

4.1.2.4. Synthesis of alkynyl-PAMAM dendrimer (10). To a solution of PAMAM dendrimer G1 (80 mg, 56 μmol) in 1 mL was added 4-pentynoic acid (132 mg, 1.4 mmol) and DMTMM (775 mg, 2.8 mmol). The mixture was stirred at rt for 12 h. The solution was purified by Superdex<sup>TM</sup> 30 increase size exclusion chromatography column to give of biotinylated PAMAM 10 as a white solid (99 mg, 86 %). <sup>1</sup>H NMR (800 MHz, <sup>2</sup>H<sub>2</sub>O) δ 3.24 (ddd, J = 24.0, 14.8, 6.3 Hz, 40H), 2.73 (t, J = 7.3 Hz, 24H), 2.56–2.52 (m, 12H), 2.40 (t, J = 7.1 Hz, 16H), 2.34 (dt, J = 21.5, 7.0 Hz, 40H). <sup>13</sup>C NMR (200 MHz, <sup>2</sup>H<sub>2</sub>O) δ 174.77, 174.62, 174.25, 173.93, 170.86, 82.46, 69.4, 61.88, 60.04, 55.19, 50.91, 49.73, 48.85, 48.72, 39.53, 38.54, 38.29, 36.5, 34.3, 32.38, 32.26, 14.37. ESI-HRMS calcd. for  $C_{102}H_{161}N_{29}O_{20}$  ([M + H]<sup>+</sup>) 2070.2375, found 2070.2474.

4.1.2.5. General procedure A for Cu(I)-catalyzed azide-alkyne cycloaddition (CuAAC). To a solution of sialyllactose derivatives (6 or 7, 2  $\mu$ mol) and PAMAM dendrimer (9 or 10, 0.1  $\mu$ mol) in 200  $\mu$ L water was added THPTA (3  $\mu$ mol), CuSO<sub>4</sub>·5H<sub>2</sub>O (1  $\mu$ mol) and sodium L-ascorbate (2  $\mu$ mol). The resulting solution was stirred vigorously for 24 h at rt and then filtered through filters of 0.45  $\mu$ m pore size. The purification was performed on a Superdex<sup>TM</sup> 30 increase size exclusion chromatography column.

4.1.2.6. Synthesis of biotinylated multivalent 9-O-acetylated-6'-sialyllatose-PAMAM dendrimer (1). Prepared from biotinylated alkynyl-PAMAM dendrimer 9 (0.28 mg, 0.1  $\mu$ mol) and 9-O-acetylated 6'-sialyllatosyl azide 7 (1.4 mg, 2  $\mu$ mol) according to general procedure A to give 1 as a white solid (0.71 mg, 91 %).  $^{1}$ H NMR (800 MHz,  $^{2}$ H<sub>2</sub>O)  $\delta$  7.80 (s, 7H), 5.50 (d, J = 9.2 Hz, 7H), 4.23 (d, J = 7.9 Hz, 7H), 4.16 (d, J = 11.3 Hz,7H), 3.98 (s, 7H), 3.94 (dd, J = 11.8, 5.8 Hz, 7H), 3.90–3.85 (m, 7H), 3.80 (d, J = 8.6 Hz, 7H), 3.75 (t, J = 9.4 Hz, 7H), 3.69 (d, J = 4.0 Hz, 7H), 3.65-3.58 (m, 14H), 3.54-3.34 (m, 100H), 3.31 (td, J = 13.3, 11.8, 7.5 Hz, 14H), 3.02 (d, J = 33.5 Hz, 28H), 2.76 (t, J = 7.8 Hz, 8H), 2.55 (s, 14H), 2.2.5–2.4 (m, 7H), 2.35 (q, J = 8.5, 7.9 Hz, 16H), 2.22–2.06 (m, 24H), 1.87 (s, 21H), 1.76 (s, 21H), 1.14–0.96 (m, 7H). <sup>13</sup>C NMR (200 MHz, <sup>2</sup>H<sub>2</sub>O) 174.83, 174.49, 174.11, 173.31, 170.86, 146.45, 122.15, 103.04, 100, 86.85, 78.42, 77.26, 74.5, 73.57, 72.05, 71.82, 71.65, 71.52, 70.49, 69.38, 69.23, 69.04, 68.33, 68.2, 68.07, 65.4, 63.61, 63.36, 62.19, 60.1, 59.59, 51.52, 48.7, 39.92, 38.42, 38.28, 34.84, 21.86, 20.89, 20.06. ESI-HRMS calcd. for  $C_{317}H_{534}N_{57}O_{167}S$  ([M - H]<sup>-</sup>) 7843.4771, found 7843.4611.

4.1.2.7. Synthesis of multivalent 9-O-acetylated-6'-sialyllatose-PAMAM dendrimer (2). Prepared from alkynyl-PAMAM dendrimer 10 (0.21 mg, 0.1 µmol) and 9-O-acetylated 6'-sialyllatosyl azide 7 (1.4 mg, 2 µmol) according to general procedure A to give 2 as a white solid (0.74 mg, 94 %).  $^1\mathrm{H}$  NMR (800 MHz,  $^2\mathrm{H}_2\mathrm{O}$ )  $\delta$  7.96 (s, 8H), 5.71–5.61 (m, 8H), 4.41 (t, J=6.2 Hz, 8H), 4.36–4.31 (m, 8H), 4.12 (dt, J=11.8, 5.2 Hz, 8H), 4.08–4.01 (m, 8H), 3.97 (s, 8H), 3.94–3.85 (m, 16H), 3.78 (d, J=25.1 Hz, 20H), 3.67 (d, J=11.0 Hz, 8H), 3.63–3.47 (m, 32H), 3.25–3.11 (m, 24H), 2.93 (d, J=6.3 Hz, 8H), 2.71 (s, 30H), 2.57–2.48 (m, 16H), 2.38–2.27 (m, 16H), 2.04 (s, 21H), 1.94 (s, 21H), 1.67 (td, J=12.4, 12.0, 6.5 Hz, 8H).  $^{13}\mathrm{C}$  NMR (200 MHz,  $^2\mathrm{H}_2\mathrm{O}$ )  $\delta$  174.87, 174.77, 174.34, 173.43, 171.03, 161.33, 157.71, 156.38, 146.72, 122.38, 103.26, 100.28, 87.05, 78.68, 77.47, 74.73, 73.77, 72.32, 72.28, 71.85, 70.73,

69.26, 68.55, 68.35, 65.67, 63.71, 59.88, 51.75, 51.18, 49.9, 48.96, 40.13, 38.6, 38.51, 36.7, 35.02, 32.55, 32.4, 32.15, 31.92, 22.08, 21.05, 20.26. ESI-HRMS calcd. for  $C_{311}H_{515}N_{58}O_{172}S$  ([M - H]  $^-$ ) 7814.3340, found 7814.3122.

4.1.2.8. Synthesis of biotinylated multivalent 6'-sialyllatose-PAMAM dendrimer (3). Prepared from biotinylated alkynyl-PAMAM dendrimer 9 (0.28 mg, 0.1 µmol) and 6'-sialyllatosyl azide 6 (1.3 mg, 2 µmol) according to general procedure A to give 3 as a white solid (0.68 mg, 90 %). <sup>1</sup>H NMR (800 MHz, <sup>2</sup>H<sub>2</sub>O)  $\delta$  7.80 (d, J = 7.1 Hz, 7H), 5.50 (d, J = 9.2Hz, 7H), 4.23 (d, J = 7.9 Hz, 7H), 3.98 (s, 7H), 3.80 (t, J = 8.6 Hz, 7H), 3.76 (t, J = 9.3 Hz, 7H), 3.70 (q, J = 4.6 Hz, 14H), 3.68-3.58 (m, 59H), 3.52-3.41 (m, 94H), 3.41-3.35 (m, 14H), 3.34-3.28 (m, 14H), 3.02 (d, J = 37.0 Hz, 28H), 2.76 (t, J = 7.8 Hz, 16H), 2.82-2.74 (m, 14H),2.66-2.62 (m, 8H), 2.54-2.48 (m, 16H), 2.45-2.40 (m, 9H), 2.38-2.31 (m, 17H), 1.92 (s, 21H), 1.66 (t, J = 12.2 Hz, 7H), 1.05 (s, 41H). <sup>13</sup>C NMR (200 MHz,  ${}^{2}\text{H}_{2}\text{O}$ )  $\delta$  174.55, 174.06, 173.33, 146.47, 122.14, 103.05, 99.99, 86.86, 78.4, 77.25, 74.53, 73.51, 73.16, 72.31, 72.08, 71.82, 71.67, 70.52, 69.39, 68.28, 68.19, 68.11, 63.45, 62.34, 62.2, 60.11, 59.61, 54.34, 51.54, 48.72, 39.91, 38.43, 38.3, 32.25, 21.88, 20.86, 19.59. ESI-HRMS calcd. for  $C_{303}H_{520}N_{57}O_{160}S$  ([M - H]<sup>-</sup>) 7549.4032, found 7549.4001.

4.1.2.9. Synthesis of multivalent 6'-sialyllatose-PAMAM dendrimer (4). Prepared from alkynyl-PAMAM dendrimer 10 (0.21 mg, 0.1 µmol) and 6'-sialyllatosyl azide 6 (1.3 mg, 2 µmol) according to general procedure A to give 4 as a white solid (0.7 mg, 92 %).  $^1\mathrm{H}$  NMR (800 MHz,  $^2\mathrm{H}_2\mathrm{O})$   $\delta$  7.96 (d, J=7.5 Hz, 8H), 5.65 (d, J=9.2 Hz, 8H), 4.40 (d, J=7.8 Hz, 8H), 3.99–3.94 (m, 7), 3.93–3.89 (m, 8H), 3.88–3.84 (m, 10H), 3.83–3.74 (d, J=10.2 Hz, 34H), 3.65–3.62 (m, 8H), 3.61–3.52(m, 22H), 3.51–3.44 (m, 16H), 3.19–3.13 (m, 20H), 2.93 (t, J=7.0 Hz, 14H), 2.66–2.62 (m, 8H), 2.51 (t, J=7.6 Hz, 18H), 1.94 (d, J=16.1 Hz, 24H), 1.74–1.61 (m, 8H).  $^{13}\mathrm{C}$  NMR (200 MHz,  $^2\mathrm{H}_2\mathrm{O})$   $\delta$  175.00, 174.79, 173.43, 146.71, 122.30, 103.21, 100.24, 87.04, 78.62, 77.47, 74.74, 73.71, 72.49, 72.32, 71.81, 70.75, 69.56, 68.50, 68.33, 63.58, 62.61, 59.87, 51.76, 49.02, 40.09, 38.63, 38.47, 35.02, 22.04, 21.05. ESI-HRMS calcd. for  $\mathrm{C}_{295}\mathrm{H}_{499}\mathrm{N}_{58}\mathrm{O}_{164}$  ([M - H]  $^-$ ) 7478.2495, found 7478.2260.

4.2. SPR kinetic measurements of multivalent sialyllacosyl PAMAM dendrimer analogs with SARS-CoV-2 spike protein and HA protein (A/Hong Kong/1/1968 stain)

#### 4.2.1. General information

SARS-CoV-2 spike protein (wild type (wt), Omicron BA4 mutant and Omicron BA5 mutant) and HA protein of A/Hong Kong/1/1968 IVA stain were purchased from Sino Biological (Wayne, PA, USA). Sensor SA chips (with pre-immobilized streptavidin) were from BIAcore (GE Healthcare, Uppsala, Sweden). SPR measurements were performed on a BIAcore T200 operated using BIAcore T200 control and BIAevaluation software (Biacore T200 Evaluation version 3.2.1, GE Healthcare, Uppsala, Sweden).

## 4.2.2. Immobilization of multivalent sialyllactose PAMAM dendrimers on SA censor chip

The biotinylated multivalent sialyllactose PAMAM dendrimer 1 and 3 (200 µg/mL) were immobilized to a streptavidin (SA) chip based on the manufacturer's protocol. In brief, a 20 µL solution of the bitinylated multivalent sialyllactose PAMAM dendrimers (0.1 mg/mL) in HBS-EP buffer (0.01 M HEPES, 0.15 M NaCl, 3 mM EDTA, 0.005 % surfactant P20, pH 7.4) was injected over flow cell 2 (FC2), 3 (FC3) and 4 (FC4) of the SA chip at a flow rate of 10 µL/min. The successful immobilization of dendrimers was confirmed by the observation of a  $\sim\!800$  resonance unit (RU) increase in the sensor chip. The control flow cell (FC1) was prepared by 1 min injection with saturated biotin.

4.2.3. Kinetic measurement of interaction between SARS-CoV-2 spike protein, HA protein and sialyllactose-conjugated dendrimers using BIAcore

SARS-CoV-2 spike protein (wt, Omicron BA4 mutant and Omicron BA5 mutant) and HA proteins of HA were diluted in HBS-EP plus buffer (0.01 M HEPES, 0.15 M NaCl, 3 mM EDTA, 0.005 % surfactant P20, pH 7.4). Different dilutions of proteins were injected at a flow rate of 30  $\mu L/$  min. At the end of the sample injection, the same buffer was flowed over the sensor surface to facilitate dissociation. After a 3 min dissociation time, the sensor surface was regenerated by injecting with 30  $\mu L$  2 M NaCl aqueous fully regenerate the surface. The response was monitored as a function of time (sensorgram) at 25 °C.

#### CRediT authorship contribution statement

Conceptualization, R.J.L.; methodology, P.H, F.Z.; analysis, P.H, K.X. Y.S; resource, R.T, R.C; original draft preparation, P.H; review and editing, F.Z. and R.J.L.; revision, P.H.,F.Z. and R.J.L., funding acquisition, F.Z. and R.J.L. All authors have read and agreed to the published version of the manuscript.

#### **Declaration of competing interest**

The authors declare that they have no known competing financial interests or personal relationships that could have appeared to influence the work reported in this paper.

#### Data availability

Data will be made available on request.

#### Acknowledgement

This research was funded by grants from the National Institutes of Health in the forms of grants S100D028523 (F. Z. and R. J. L.), AI156573 (F. Z. and R. J. L.), and the National Science Foundation GlycoMIP DMR 1933525 (F. Z. and R. J. L.).

#### Appendix A. Supplementary data

Supplementary data to this article can be found online at https://doi.org/10.1016/j.ijbiomac.2023.125714.

#### References

- [1] S.P. Otto, T. Day, J. Arino, C. Colijn, J. Dushoff, M. Li, S. Mechai, G. Van Domselaar, J. Wu, D.J.D. Earn, N.H. Ogden, The origins and potential future of SARS-CoV-2 variants of concern in the evolving COVID-19 pandemic, Curr. Biol. 31 (14) (2021) R918–R929, https://doi.org/10.1016/j.cub.2021.06.049.
- [2] R.K. Mohapatra, S. Kuppili, T. Kumar Suvvari, V. Kandi, A. Behera, S. Verma, Kudrat-E-Zahan, S.K. Biswal, T.H. Al-Noor, M.M. El-ajaily, Ashish K. Sarangi, K. Dhama, SARS-CoV-2 and its variants of concern including Omicron: a never ending pandemic, Chem. Biol. Drug Des. 99 (5) (2022) 769–788, https://doi.org/ 10.1111/cbdd.14035.
- [3] C. Willyard, What the Omicron wave is revealing about human immunity, Nature 602 (7895) (2022) 22–25.
- [4] A. Gordon, A. Reingold, The burden of influenza: a complex problem, Curr. Epidemiol. Rep. 5 (1) (2018) 1–9, https://doi.org/10.1007/s40471-018-0136-1.
- M. Javanian, M. Barary, S. Ghebrehewet, V. Koppolu, V. Vasigala, S. Ebrahimpour, A brief review of influenza virus infection, J. Med. Virol. 93 (8) (2021) 4638–4646, https://doi.org/10.1002/jmv.26990.
- [6] A. Subramanian, K. Nirantharakumar, S. Hughes, P. Myles, T. Williams, K. M. Gokhale, T. Taverner, J.S. Chandan, K. Brown, N. Simms-Williams, A.D. Shah, M. Singh, F. Kidy, K. Okoth, R. Hotham, N. Bashir, N. Cockburn, S.I. Lee, G. M. Turner, G.V. Gkoutos, O.L. Aiyegbusi, C. McMullan, A.K. Denniston, E. Sapey, J. M. Lord, D.C. Wraith, E. Leggett, C. Iles, T. Marshall, M.J. Price, S. Marwaha, E. H. Davies, L.J. Jackson, K.L. Matthews, J. Camaradou, M. Calvert, S. Haroon, Symptoms and risk factors for long COVID in non-hospitalized adults, Nat. Med. 28 (8) (2022) 1706–1714. https://doi.org/10.1038/s41591-022-01909-w.
- [7] R.K. Lim, R. Rosentreter, Y. Chen, R. Mehta, G. McLeod, M. Wan, J.D. Krett, Y. Mahjoub, A. Lee, I. Schwartz, L. Metz, L. Richer, E. Smith, M.D. Hill, R.K. Lim, L. Metz, M.D. Hill, A. Ganesh, L. Richer, I. Schwartz, A. Ganesh, A.H.C.-. Collaborators, Quality of life, respiratory symptoms, and health care utilization 1

- year following outpatient management of COVID-19: a prospective cohort study, Sci. Rep. 12 (1) (2022) 12988, https://doi.org/10.1038/s41598-022-17243-7.
- [8] A. Sarker, Z. Gu, L. Mao, Y. Ge, D. Hou, J. Fang, Z. Wei, Z. Wang, Influenza-existing drugs and treatment prospects, Eur. J. Med. Chem. 232 (2022), 114189, https://doi.org/10.1016/j.ejmech.2022.114189.
- [9] M. Liu, L.Z.X. Huang, A.A. Smits, C. Büll, Y. Narimatsu, F.J.M. van Kuppeveld, H. Clausen, C.A.M. de Haan, E. de Vries, Human-type sialic acid receptors contribute to avian influenza A virus binding and entry by hetero-multivalent interactions, Nat. Commun. 13 (1) (2022) 4054, https://doi.org/10.1038/s41467-022-31840-0.
- [10] L. Byrd-Leotis, N. Jia, Y. Matsumoto, D. Lu, Y. Kawaoka, D.A. Steinhauer, R. D. Cummings, Sialylated and sulfated N-Glycans in MDCK and engineered MDCK cells for influenza virus studies, Sci. Rep. 12 (1) (2022) 12757, https://doi.org/10.1038/s41598-022-16605-5.
- [11] T. Koley, S. Madaan, S.R. Chowdhury, M. Kumar, P. Kaur, T.P. Singh, A. S. Ethayathulla, Structural analysis of COVID-19 spike protein in recognizing the ACE2 receptor of different mammalian species and its susceptibility to viral infection, 3 Biotech 11 (2) (2021) 109, https://doi.org/10.1007/s13205-020-02599-2.
- [12] L. Yan, Y. Song, K. Xia, P. He, F. Zhang, S. Chen, R. Pouliot, D.J. Weiss, R. Tandon, J.T. Bates, D.R. Ederer, D. Mitra, P. Sharma, A. Davis, R.J. Linhardt, Heparan sulfates from bat and human lung and their binding to the spike protein of SARS-CoV-2 virus, Carbohydr. Polym. 260 (2021), 117797, https://doi.org/10.1016/j.carbool.2021.117707
- [13] L. Nguyen, K.A. McCord, D.T. Bui, K.M. Bouwman, E.N. Kitova, M. Elaish, D. Kumawat, G.C. Daskhan, I. Tomris, L. Han, P. Chopra, T.-J. Yang, S.D. Willows, A.L. Mason, L.K. Mahal, T.L. Lowary, L.J. West, S.-T.D. Hsu, T. Hobman, S. M. Tompkins, G.-J. Boons, R.P. de Vries, M.S. Macauley, J.S. Klassen, Sialic acid-containing glycolipids mediate binding and viral entry of SARS-CoV-2, Nat. Chem. Biol. 18 (1) (2022) 81–90, https://doi.org/10.1038/s41589-021-00924-1.
- [14] W. Li, R.J.G. Hulswit, I. Widjaja, V.S. Raj, R. McBride, W. Peng, W. Widagdo, M. A. Tortorici, B. van Dieren, Y. Lang, J.W.M. van Lent, J.C. Paulson, C.A.M. de Haan, R.J. de Groot, F.J.M. van Kuppeveld, B.L. Haagmans, B.-J. Bosch, Identification of sialic acid-binding function for the Middle East respiratory syndrome coronavirus spike glycoprotein, Proc. Natl. Acad. Sci. 114 (40) (2017) E8508–E8517, https://doi.org/10.1073/pnas.1712592114.
- [15] M.A. Tortorici, A.C. Walls, Y. Lang, C. Wang, Z. Li, D. Koerhuis, G.-J. Boons, B.-J. Bosch, F.A. Rey, R.J. de Groot, D. Veesler, Structural basis for human coronavirus attachment to sialic acid receptors, Nat. Struct. Mol. Biol. 26 (6) (2019) 481–489, https://doi.org/10.1038/s41594-019-0233-y.
- [16] C. Dhar, A. Sasmal, S. Diaz, A. Verhagen, H. Yu, W. Li, X. Chen, A. Varki, Are sialic acids involved in COVID-19 pathogenesis? Glycobiology 31 (9) (2021) 1068–1071, https://doi.org/10.1093/glycob/cwab063.
- [17] A.N. Baker, S.-J. Richards, C.S. Guy, T.R. Congdon, M. Hasan, A.J. Zwetsloot, A. Gallo, J.R. Lewandowski, P.J. Stansfeld, A. Straube, M. Walker, S. Chessa, G. Pergolizzi, S. Dedola, R.A. Field, M.I. Gibson, The SARS-COV-2 spike protein binds sialic acids and enables rapid detection in a lateral flow point of care diagnostic device, ACS Central Sci. 6 (11) (2020) 2046–2052, https://doi.org/ 10.1021/acscentsci.0c00855.

- [18] S.J.L. Petitjean, W. Chen, M. Koehler, R. Jimmidi, J. Yang, D. Mohammed, B. Juniku, M.L. Stanifer, S. Boulant, S.P. Vincent, D. Alsteens, Multivalent 9-Oacetylated-sialic acid glycoclusters as potent inhibitors for SARS-CoV-2 infection, Nat. Commun. 13 (1) (2022) 2564, https://doi.org/10.1038/s41467-022-30313-8.
- [19] A. Kumar, R. Parashar, S. Kumar, M.A. Faiq, C. Kumari, M. Kulandhasamy, R. K. Narayan, R.K. Jha, H.N. Singh, P. Prasoon, S.N. Pandey, K. Kant, Emerging SARS-CoV-2 variants can potentially break set epidemiological barriers in COVID-19, J. Med. Virol. 94 (4) (2022) 1300–1314, https://doi.org/10.1002/jmv.27467.
- [20] R.J. Oidtman, P. Arevalo, Q. Bi, L. McGough, C.J. Russo, D. Vera Cruz, M. Costa Vieira, K.M. Gostic, Influenza immune escape under heterogeneous host immune histories, Trends Microbiol. 29 (12) (2021) 1072–1082, https://doi.org/10.1016/j. tim. 2021.05.009
- [21] S.-J. Kwon, D.H. Na, J.H. Kwak, M. Douaisi, F. Zhang, E.J. Park, J.-H. Park, H. Youn, C.-S. Song, R.S. Kane, J.S. Dordick, K.B. Lee, R.J. Linhardt, Nanostructured glycan architecture is important in the inhibition of influenza A virus infection, Nat. Nanotechnol. 12 (1) (2017) 48–54, https://doi.org/10.1038/nnano.2016.181
- [22] S.C. Günther, J.D. Maier, J. Vetter, N. Podvalnyy, N. Khanzhin, T. Hennet, S. Stertz, Antiviral potential of 3'-sialyllactose- and 6'-sialyllactose-conjugated dendritic polymers against human and avian influenza viruses, Sci. Rep. 10 (1) (2020) 768, https://doi.org/10.1038/s41598-020-57608-4.
- [23] K. Villadsen, M.C. Martos-Maldonado, K.J. Jensen, M.B. Thygesen, Chemoselective reactions for the synthesis of glycoconjugates from unprotected carbohydrates, ChemBioChem 18 (7) (2017) 574–612, https://doi.org/10.1002/cbic.201600582.
- [24] A.J. Fairbanks, Applications of Shoda's reagent (DMC) and analogues for activation of the anomeric centre of unprotected carbohydrates, Carbohydr. Res. 499 (2021), 108197, https://doi.org/10.1016/j.carres.2020.108197.
- [25] J. Rauvolfova, A. Venot, G.-J. Boons, Chemo-enzymatic synthesis of C-9 acetylated sialosides, Carbohydr. Res. 343 (10) (2008) 1605–1611, https://doi.org/10.1016/ i.carres.2008.05.002.
- [26] A.-M.T. Baumann, M.J.G. Bakkers, F.F.R. Buettner, M. Hartmann, M. Grove, M. A. Langereis, R.J. de Groot, M. Mühlenhoff, 9-O-acetylation of sialic acids is catalysed by CASD1 via a covalent acetyl-enzyme intermediate, Nat. Commun. 6 (1) (2015) 7673, https://doi.org/10.1038/ncomms8673.
- [27] H. Ogura, K. Furuhata, S. Sato, K. Anazawa, M. Itoh, Y. Shitori, Synthesis of 9-O-acyl- and 4-O-acetyl-sialic acids, Carbohydr. Res. 167 (1987) 77–86, https://doi.org/10.1016/0008-6215(87)80269-0.
- [28] L. Liang, D. Astruc, The copper(I)-catalyzed alkyne-azide cycloaddition (CuAAC) "click" reaction and its applications. An overview, Coord. Chem. Rev. 255 (23) (2011) 2933–2945, https://doi.org/10.1016/j.ccr.2011.06.028.
- [29] D. Schulz, A. Rentmeister, Current approaches for RNA labeling in vitro and in cells based on click reactions, ChemBioChem 15 (16) (2014) 2342–2347, https://doi. org/10.1002/cbic.201402240.
- [30] P. Pattnaik, Surface plasmon resonance, Appl. Biochem. Biotechnol. 126 (2) (2005) 79–92. https://doi.org/10.1385/ABAB:126:2:079.
- [31] Y.-J. Li, L.-J. Bi, X.-E. Zhang, Y.-F. Zhou, J.-B. Zhang, Y.-Y. Chen, W. Li, Z.-P. Zhang, Reversible immobilization of proteins with streptavidin affinity tags on a surface plasmon resonance biosensor chip, Anal. Bioanal. Chem. 386 (5) (2006) 1321–1326, https://doi.org/10.1007/s00216-006-0794-6.